Atomic layer diffusion and electronic structure at $In_{0.53}Ga_{0.47}As/InP$ interfaces

P. E. Smith[a)]
Department of Physics, The Ohio State University, 2015 Neil Avenue, Columbus, Ohio 43210

S. H. Goss, S. T. Bradley, M. K. Hudait, Y. Lin, and S. A. Ringel
Department of Electrical Engineering, The Ohio State University, 2015 Neil Avenue, Columbus, Ohio 43210

L. J. Brillson
Department of Physics and Electrical Engineering, The Ohio State University, 2015 Neil Avenue, Columbus, Ohio 43210

(Received 13 June 2003; accepted 5 January 2004; published 25 February 2004)

We have used secondary ion mass spectrometry and cathodoluminescence spectroscopy to determine the effects that growth and postgrowth conditions have on interdiffusion and near band edge emissions in $In_{0.53}Ga_{0.47}As/InP$ heterojunctions grown by molecular beam epitaxy. This lattice-matched interface represents a model system for the study of atomic movements and electronic changes with controlled anion overlap during growth. Structures subjected to anneals ranging from 440 to 495 °C provide a quantitative measure of concentration-driven cross diffusion of group-III and group-V atoms. By measuring anneal-induced broadening at the InGaAs-on-InP interface we have determined an activation energy for As diffusion into InP of $\sim 2.44 \pm 0.40$ eV. An interface layer with Ga–P bonds indicates Ga competes favorably versus As for bonding in the preannealed InP near-surface region. In addition, we present evidence that interface chemical effects manifest themselves electronically as variations of the InGaAs band gap energy. © *2004 American Vacuum Society.* [DOI: 10.1116/1.1651112]

I. INTRODUCTION

The $In_{0.53}Ga_{0.47}As/InP$ material system has been the focus of much research because of its importance in low band gap optoelectronic applications including infrared photosensors and thermophotovoltaics. It is difficult to achieve abrupt interfaces in these structures because both group-III and group-V elements must be switched at the interface. A high flux ratio of group-V to group-III elements is necessary for low defect densities and is maintained during source switching by allowing time for the new group-V element to establish in the chamber before closing the previous group-V source and starting growth of subsequent layers. Along with minimizing chamber memory effects, this allows the new group-V element time to diffuse into the existing epilayer, possibly resulting in interfacial broadening. Previous work[1–3] reported the presence of several monolayers of As replacement of P, which could be removed by subsequent exposure to P.[4] It has been postulated for metalorganic vapor phase epitaxy grown heterostructures that early in growth, As–P exchange occurs during a short time ($\sim$10 s).[5] Beyond that point, As slowly migrates into InP, creating a highly strained InAsP layer.[5] Others, citing Raman data,[6,7] have reported evidence of P incorporation into the InGaAs lattice at growth or anneal temperatures above 640 °C. Several authors have studied the effect of such high-temperature anneals on diffusion in similar structures.[5,8–15] The general consensus is that vacancies, both grown-in and thermally generated, play an important role in diffusion on both sublattices. An activation energy of 1.7 eV was reported for diffusion on both undoped group-III and group-V sublattices.[5,9] However, at the high temperatures (>500 °C) most of these studies employ, P outdiffusion from the bulk will be significant,[16,17] resulting in some quenching of vacancies. Our study is of undoped molecular beam epitaxy (MBE) grown InGaAs/InP heterojunctions with varying As exposures systematically exposed to sub-500 °C anneals for long (>30 min) intervals. The latter simulates annealing treatments that might be experienced by device structures. The nature of diffusion and interfacial reactions at such interfaces is a critical issue since these chemical effects may introduce defects and alter band offsets, adversely affecting device performance.

II. EXPERIMENT

Five $InP/In_{0.53}Ga_{0.47}As/InP$ double heterostructures were grown on semi-insulating Fe-doped (100) InP substrates with no ($<\pm 0.2°$) miscut by solid source MBE with valved cracker sources for arsenic and phosphorus: Prior to being loaded into the growth chamber epiready InP wafers are subject to a 60 min. 300 °C anneal under a pressure of 5×10^{-9} Torr to remove water vapor. Substrate oxide desorption is done in the growth chamber at a temperature of 510 °C under a P overpressure of 1×10^{-5} Torr and confirmed by a (2×4) reflection high energy electron diffraction pattern indicating a clean (100) InP surface. After oxide desorption growth takes place at 485 °C using group-V:group-III beam pressure ratios of 24:1 for InGaAs and 12:1 for InP. Growth rates are 1.743 and 3.18 A/s for InP and InGaAs,

[a)]Author to whom correspondence should be addressed; electronic mail: psmith@pacific.mps.ohio-state.edu

TABLE I. Growth sequence for InP/InGaAs/InP double heterostructures. Time proceeds from top to bottom.

Sources	Time
In and P sources opened	200 nm at 0.174 nm/s
In closed, As and P held open	20 s
P closed, As held open	20–150 s
In, Ga, and As held open	500 nm at 0.318 nm/s
In and Ga closed, As and P opened	20 s
As closed, P held open	20 s
In and P sources opened	50 nm at 0.174 nm/s
All sources closed	

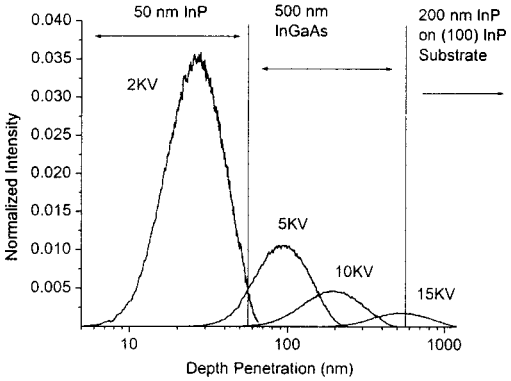

FIG. 1. Electron depth penetration for beam energies showing selective excitation for the energies used.

respectively. The growth sequence for these heterostructures is outlined in Table I. Beginning at the substrate, the layers are 200 nm InP, 500 nm $In_{0.53}Ga_{0.47}As$, and 50 nm InP. The samples differ in the amount of time As_2 is allowed to establish (''dwell'' time) in the chamber between finishing InP and beginning $In_{0.53}Ga_{0.47}As$ growth at the InGaAs-on-InP interface. Growth at the InP-on-InGaAs interface is identical in all five samples. After initial analysis, samples were annealed at temperatures of 440, 460, and 495 °C for 3000 s in ultrahigh vacuum (UHV) as measured by an E2T Pulsar II 7000EH-2 optical pyrometer focused through a quartz window onto a Mo sample mount, noting an error of ± 10 °C. The radiative cooling time constant of the heating mount is 65 s, indicating a fast cooling relative to the anneal time. Chamber background pressure while annealing is 5×10^{-10} Torr.

Negative ion secondary ion mass spectrometry (SIMS) is performed on a PHI TRIFT-III time-of-flight SIMS using 1 keV Cs^+ beam energy. The analysis beam is a 15 keV isotopically pure focused ^{69}Ga ion beam. Background pressure during analysis is 2×10^{-9} Torr. Typical analysis time is approximately 1 h/sample.

Cathodoluminescence spectroscopy (CLS) is performed using a JEOL JAMP-7800F UHV scanning electron microscope as the electron-beam source. Optical emissions are collected via an Oxford MonoCL system consisting of a parabolic mirror set in UHV and focusing collected light though a sapphire window at the vacuum–air interface. Emissions are measured using an Edinburgh Instruments high-purity germanium detector. CLS measurements are performed at temperatures of 10 K using a constant beam power of 40 μW. The electron beam is rastered over an area of 100 μm^2 during analysis. Monochromator slit width was kept constant at 0.5 mm to maintain spectral resolution at 1 nm. The CLS with variable incident beam energy provided an ability to selectively excite electron–hole pairs that recombine at different depths. This is illustrated in Fig. 1 by a Monte Carlo simulation[18] showing primary electron penetration versus beam energy for the $InP/In_{0.53}Ga_{0.47}As/InP$ double heterostructures reported here. The simulation shows that a beam energy of 5 keV will induce excitation localized near the InP-on-InGaAs interface, while a beam energy of 15 keV generates excitation localized at the InGaAs-on-InP interface. Recombination induced by an intermediate energy, 10 keV beam, will be localized within the 500 nm InGaAs layer. Achieving high signal-to-noise ratios and nondestructive current levels while maintaining the constant power condition limited our primary beam energy to 5 keV or higher. Monte Carlo simulations show that the difference in excitation depth for 4 and 5 keV electrons is approximately 20 nm, i.e., within the diffusion length of free carriers. Excitation from a 3 keV beam is maximized within the 50 nm InP cap layer and results in much lower recombination in the InGaAs layer. The sputter depth rates vary by up to 50% from profile to profile. In order to compare depth profiles of intensities versus sputter depth, we normalized the depth scales to the beginning of the decrease of the InGaAs-on-InP interface As profile from its bulk value. The normalized profiles provide a relative measure of interface broadening. Determining the actual direction of broadening requires an interface marker, for which the results are presented as well.

III. RESULTS

Figure 2 shows SIMS profiles of As and P-containing fragments for the InP/InGaAs/InP heterostructures with As dwell times of (a) 40 and (b) 170 s. Both depth profiles illustrate constant As, In–As, Ga–As, and In–P intensities within each of the layers, indicating good growth uniformity and low contamination. Both profiles also display InP-on-InGaAs interface profiles that are abrupt to within the sputter-induced broadening ($<$15 nm) of the ion beam. This interface width is evident from the various In–As, P, Ga–As, and As profile widths at this interface. On the other hand, the InGaAs-on-InP interface displays profiles whose width depends on As dwell time. Figure 2(b) shows a broader such interface than Fig. 2(a) as a result of longer As dwell time. Furthermore, this broadening occurs preferentially toward the InP side of the junction.

Figure 3 illustrates the striking difference in InGaAs-on-InP interface broadening due to As dwell time. The InGaAs-on-InP interface shown in Fig. 3(a) displays systematic increases in transition region width as a function of As dwell time. In contrast, Fig. 3(b) illustrates only minor changes in interface profiles of P and As with a constant (20 s) As dwell time at the corresponding InP-on-InGaAs interfaces. Neglecting the effects of sputter-induced broadening, which

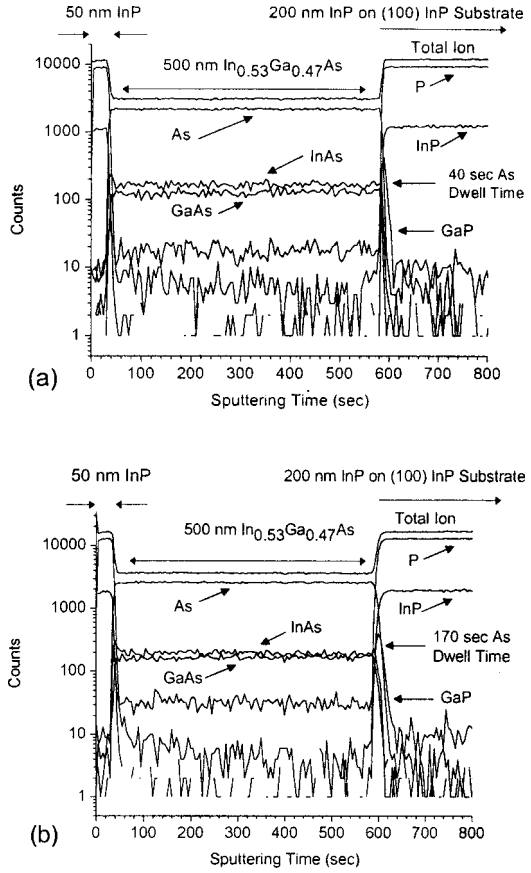

FIG. 2. SIMS sputter depth profiles showing As and P compounds in samples with 40 and 170 s As dwell time. The 170 s dwell time produces a broader interface.

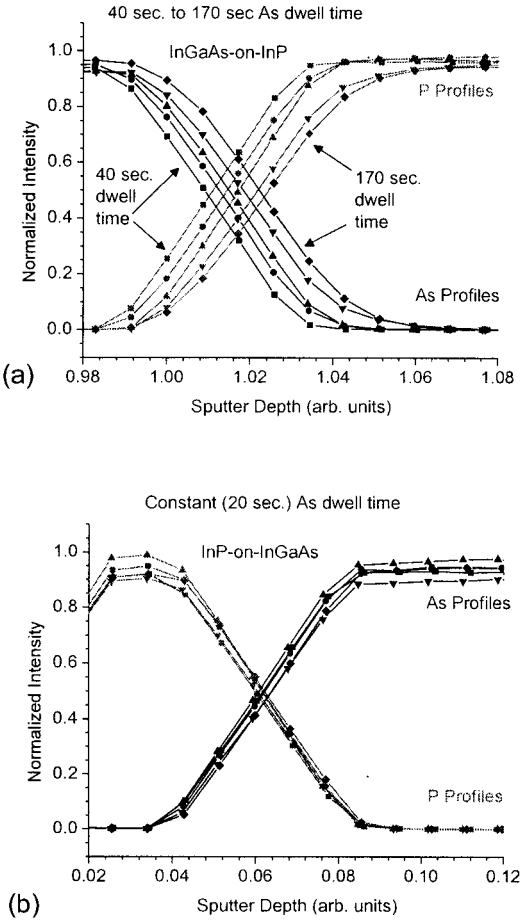

FIG. 3. Normalized depth profiles for (a) InGaAs-on-InP and (b) InP-on-InGaAs interfaces. Varying As dwell times at the InGaAs-on-InP interface (a) of 40, 80, 110, 140, and 170 s are shown from left to right. Broadening is evident for the InGaAs-on-InP (deeper) interface with varying As dwell time in (a) vs constant 20 s dwell time for all corresponding InP-on-InGaAs (shallower) interfaces in (b).

will be considered quantitatively later, and defining the transition region as the distance over which the As profile falls to $1/e$ of its bulk value, the interfaces range from ~20 to 28 nm as As dwell time increases from 40 to 170 s. We observe no saturation in As diffusion in Fig. 3(a) at dwell times up to 170 s, i.e., the interface width continues to increase with As dwell time.

Figure 4 shows the As and P profiles of the sample with an intermediate 110 s As dwell time subjected to UHV anneals at 440, 460, and 495 °C for 3000 s. The transition region broadens from ~20 to 75 nm as the sample is annealed. From the annealed-sample SIMS profiles we may extract activation energies and diffusion coefficients for the process. Assuming a Fickian model with constant source concentration, the differential equation is given as

$$\frac{\partial^2}{\partial z^2}C(z,t)=\frac{1}{D(T)}\frac{\partial C(z,t)}{\partial t}, \tag{1}$$

where C is the As concentration, z is depth, t is the anneal time, and $D(T)$ is a temperature-dependent diffusion coefficient given by

$$D(T)=D_0e^{-(Q/kT)}, \tag{2}$$

where Q is the activation energy for the diffusion process, D_0 is a material-dependent prefactor, T is temperature in Kelvin, and k is the Boltzman constant. The solution to Eq. (1) with initial boundary conditions corresponding to a constant As surface concentration of half its bulk value C_0 is given by[19]

$$C(z,t)=\frac{C_0}{2}\left(1-\mathrm{erf}\left(\frac{z}{2\sqrt{Dt}}\right)\right). \tag{3}$$

The assumption of Fickian diffusion is normally only valid in an isotropic lattice. However, Fick's law has been found to accurately model diffusion on the group-V sublattice in $In_{0.66}Ga_{0.33}As/In_{0.66}Ga_{0.33}As_{0.7}P_{0.3}$ heterostructures.[9] Lattice strain can result in non-Fickian diffusion, which has been reported at sub-800 °C temperatures in InGaAs/InP quantum wells.[10] The thick InGaAs layer used in our study is highly resistant to the changes in lattice strain that would occur with differing diffusion rates on the group-III and group-V sublattices. Furthermore, the anneal times used in our study fall in the regime that Bollet *et al.*[10] attribute to Fickian diffusion.

In order to remove the effects of diffusion due to elevated growth temperatures as well as knock-on effects due to the

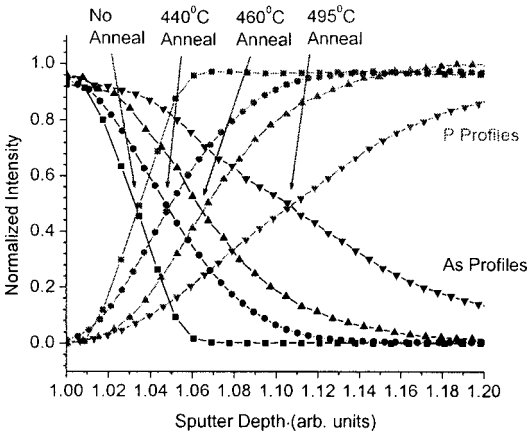

FIG. 4. InGaAs-on-InP interface exposed to 3000 s anneals at 440, 460, and 495 °C. Increasing anneal temperature increases interface broadening.

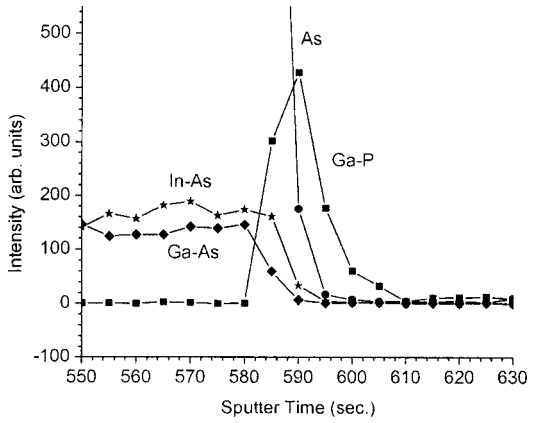

FIG. 6. Representitive SIMS profiles showing [Ga–P] extending farther into InP than [In–As] or [Ga–As] at the unannealed InGaAs-on-InP interface with 40 s As dwell time.

sputter process, the broadening observed in the nonannealed profile has been subtracted from the annealed profiles. The net As profiles are then fit to the error function solution of Fick's law. Figure 5 shows a linear fit from which $E_{act} = 2.44 \pm 0.40$ eV and $D_0 = 18.4\,cm^2/s$ were extracted. Significantly, the InP-on-InGaAs interfaces show only relatively small changes with annealing below the 485 °C growth temperature.

The SIMS process results in secondary ion ejection of not only elemental species but also fragments of molecular complexes. Neglecting complex formation resulting from the sputter process, such fragments may indicate local chemical bonding at particular depths. Indeed, SIMS reveals Ga–P bonds at both InGaAs-on-InP and InP-on-InGaAs interfaces. Recombination with the ^{69}Ga SIMS analysis beam is ruled out here by restricting our analysis to ^{71}Ga species only. Analogous to Fig. 2, Fig. 6 shows SIMS depth profiles of As, In–As, Ga–As, and Ga–P at the InGaAs-on-InP interface subject to 40 s As dwell time during growth. The Ga–P intensity profiles show only small variations for the different As dwell times. The profile shown in Fig. 6 is typical of the majority of our unannealed samples in that the Ga–P bonding profile is observed at greater depths than the profiles of As containing compounds.

The effect of annealing on the Ga–P fragment profile at the InGaAs-on-InP interfaces appears in Fig. 7. Shown here is the heterojunction with 110 s As dwell time during growth and with subsequent annealing at temperatures of 440, 460, and 495 °C. Figure 7 shows that annealing broadens the Ga–P fragment profile from an initial full width half maximum (FWHM) of 12 nm to greater than 40 nm. Furthermore, this width is asymmetric, broadening primarily into the deeper InP. The symmetric shape of this Ga–P peak in Fig. 6 indicates that broadening due to knock-on sputtering is minimal. The integrated intensity of Ga–P fragments also decreases with annealing.

Low-temperature CLS spectra, shown in Fig. 8 for the structures with 110, 140, and 170 s As dwell time, provide a measure of electronic changes due to chemical effects. Figure 1 showed how the 5, 10, and 15 keV electron beams can preferentially excite the InP-on-InGaAs interface, the $In_{0.53}Ga_{0.47}As$ layer, and the InGaAs-on-InP interface respec-

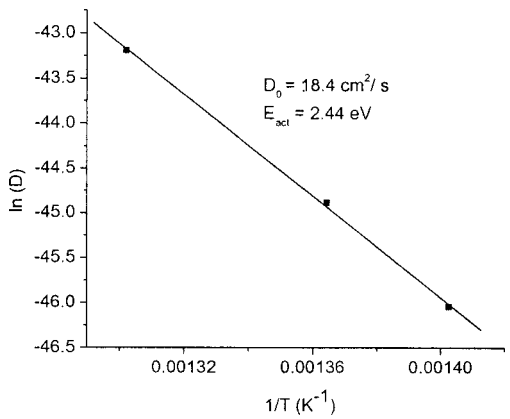

FIG. 5. Linear fit determining the Arrhenius relationship parameters E_{act} ($-$slope$*k_B$) and D_0 ($e^{(y\text{-intercept})}$) derived from measuring anneal-induced broadening at the InGaAs-on-InP interface.

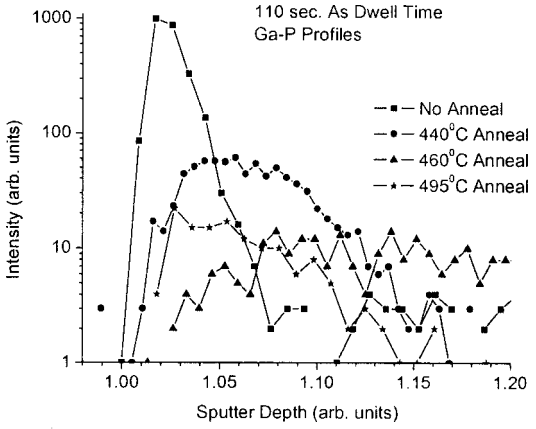

FIG. 7. InGaAs-on-InP [Ga–P] bonding depth profiles for annealed samples exposed to 110 s As dwell time. The profiles broaden asymmetrically with higher anneal temperatures towards the InP buffer layer.

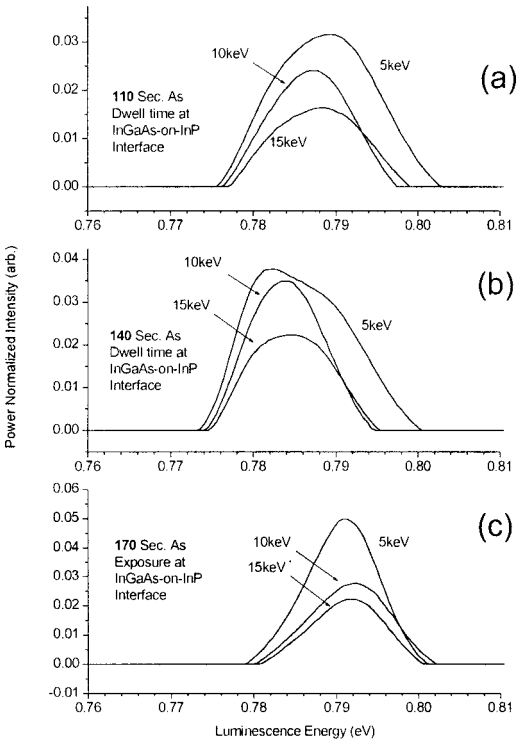

FIG. 8. 10 K depth-dependent CLS spectra showing broadening in NBE emission energy at interfaces (5 and 15 keV) relative to "bulk" (10 keV) InGaAs and overall peak shifting to higher energy with increased As dwell time.

tively. Figure 8 shows that some broadening to higher energies of the InGaAs near band edge (NBE) emission is evident for excitation at the interfaces relative to the 10 keV (bulk InGaAs) layer. For example the FWHM increases 20%–30% for the interfaces versus the bulk of the 110 s As dwell time sample and 20%–45% for the sample with 140 s As dwell time. These spectral energies and linewidths appear in Table II.

TABLE II. Peak energy and FWHM of NBE CLS emissions for samples with 110, 140, and 170 s As dwell time. In the samples with 110 and 140 s As dwell time InGaAs, FWHM is larger at the interfaces relative to the bulk. Emission energy is slightly higher and FWHM lower in the 170 s exposed sample.

Dwell time (s)	E_{beam} (keV)	E_{peak} (eV)	FWHM (eV)
110	5	0.789	0.016
110	10	0.787	0.012
110	15	0.788	0.014
140	5	0.782/0.787 (two transitions)	0.016
140	10	0.784	0.011
140	15	0.784	0.013
170	5	0.791	0.010
170	10	0.792	0.011
170	15	0.792	0.011

IV. DISCUSSION

In the nonannealed samples, the observation of As at depths exceeding the few monolayers over which As–P exchange has been previously reported to occur indicates that the observed broadening is due to diffusion of As into the InP buffer layer. The energetics of the As–P exchange reaction have been studied by a number of authors,[20–22] who have reported values of 1.2–1.6 eV for the activation energy of this reaction. Our activation energy window of 2.04–2.84 eV, derived from annealing, is close to the 1.7 eV reported for diffusion of As on the group-V sublattice.[5,9] The largest potential source of error in our calculation is in the assumption of a constant As "surface" concentration in Fick's law. This assumption requires that the 50% As–P crossover remains at a constant depth. In fact, we observe little movement of the 50% As–P crossover point after annealing relative to the Ga–P peak position, which can serve as an interface marker. This indicates that our assumption of a constant 50% As surface concentration is reasonable. Our temperature dependent diffusion coefficient $D(T)$ is found to differ significantly from those reported by Bollet *et al.*[10] when extrapolated to higher temperatures (6.4×10^{-11} versus $4\times10^{-14}\,cm^2/s$ at 800 °C). Different diffusion mechanisms or competing processes could be present due to the large difference in anneal temperature and sample structure (500 versus 10 nm respective InGaAs layers).

Figure 6 shows Ga–P bonding at greater depths than As containing fragments in the nonannealed sample with 40 s As dwell time. The Ga–P bonds at the InGaAs-on-InP interface indicate that P is competing with As for Ga early in interface growth. This is consistent with the higher thermodynamic stability of GaP (−102 kJ/mole) versus InAs (57.7 kJ/mole). Figure 7 shows that annealing broadens the Ga–P profile but does not increase the integrated fragment amount. This implies that Ga–P bonds form only during growth, and that reactive diffusion of Ga into InP is minimal. It is notable that other authors observe Ga–P bonding only after growth or anneals above 640 °C, likely due to the high energies needed to break bonds which would drive this reaction.[23] It is also significant that In–As, Ga–As, and As profiles do not show the same ratios of these compounds in the transition region during annealing. Though SIMS matrix effects could account for some of this discrepancy, it is natural to assume that the InGaAs mole fraction in the transition region changes with diffusion. The mechanism for Ga–P bonding at the InP-on-InGaAs interface may be the replacement of As by P, which is energetically slightly favorable (0.14 eV/molecule for InP relative to InAs) to replacement of P by As.[23] We observe ~2–3 times the integrated intensity of Ga–P at the InGaAs-on-InP interface relative to the InP-on-InGaAs interface. The abruptness of the InP-on-InGaAs interface with annealing compared with its counterpart may be accounted for in terms of the latter's extended As dwell time, which introduces a mixed anion sublattice [see Fig. 3(a)] that could lower the barrier for subsequent As diffusion.

The CL results in Fig. 7 and Table II are generally consistent with the chemical features provided by SIMS. The

band gap of InGaAs lattice matched to InP has been measured by photoreflectance to be 0.807 eV at 10 K.[24] We observe a slightly lower emission at approximately 0.79 eV, likely due to NBE transitions and an apparent shift from self-absorption. The Ga–P fragments found in SIMS depth profiles indicate compositional changes at both the InP-on-InGaAs and InGaAs-on-InP interfaces. Thus, in Fig. 7(a), the peak FWHM at 10 keV maximizes excitation within the InGaAs film and equals 0.012 eV, compared with 0.016 and 0.014 eV for 5 and 15 keV at the shallower and deeper interfaces, respectively. Similar behavior is evident for the peaks in Fig. 7(b), where in fact two peaks are evident for the 5 keV curve. These FWHM increases indicate less compositional homogeneity at the two InGaAs interfaces than in the ''bulk'' InGaAs film and are consistent with incorporation of P into the InGaAs lattice. The SIMS results of Fig. 3 illustrate significantly different profiles at the InGaAs-on-InP versus InP-on-InGaAs interfaces, yet the corresponding CL spectra of the two interfaces reflect more similarities than differences. On the other hand, SIMS also shows evidence for Ga–P interactions at both interfaces. These similarities rather than the differences in As dwell time may therefore be the dominant contributor to the CLS broadening. The data supports no systematic correlation between peak energy or FWHM and As dwell time. The appearance of two peaks in Fig. 7(b) and the decrease in FWHM and increase in peak energies in Fig. 7(c) could be evidence for compositional rearrangement during the extended As dwell time at the growth temperature. However, support for this speculation requires additional studies of compositional variation versus As dwell time, particularly in cross section.

V. CONCLUSIONS

We have observed systematic differences in diffusion and interfacial compound formation at the InGaAs-on-InP heterojunction interface. SIMS depth profiles reveal the presence of nanometer-scale Ga–P bonding at both preannealed InGaAs-on-InP and InP-on-InGaAs junctions. The position of Ga–P bonding within the InGaAs-on-InP interface layer profile indicates that Ga competes favorably versus As for bonding at this junction. Postannealing of these heterojunctions demonstrates that As can diffuse tens of nanometers into the InP at near-growth temperatures. Such interface changes can have significant consequences for devices. These interface diffusion and bonding phenomena can help define the role of bulk thermodynamics in atomic displacement and exchange reactions for III–V compound heterojunctions in general. Overall, the results show that atomic redistribution, bond rearrangement, and local electronic structure at a lattice-matched III–V compound heterojunction depend sensitively on the competition of atomic species in the transition region of a heterojunction during growth.

ACKNOWLEDGMENTS

This work is supported by the Department of Energy (Jane Zhu), the National Science Foundation (Verne Hess), the Office of Naval Research (Colin Wood), and the National Aeronautics and Space Administration.

[1]J. M. Moison, M. Bensoussan, and F. Houzay, Phys. Rev. B **34**, 2018 (1986).
[2]G. Hollinger, D. Gallet, M. Gendry, C. Santinelli, and P. Victorovitch, J. Vac. Sci. Technol. B **8**, 832 (1990).
[3]C. H. Li, L. Li, D. C. Law, S. B. Visbeck, and R. F. Hicks, Phys. Rev. B **65**, 205322 (2002).
[4]D. E. Aspnes, M. C. Tamargo, M. J. S. P. Brasil, R. E. Nahory, and S. A. Schwartz, Appl. Phys. Lett. **64**, 3279 (1994).
[5]D. C. Law, Y. Sun, C. H. Li, S. B. Visbeck, G. Chen, and R. F. Hicks, Phys. Rev. B **66**, 045314 (2002).
[6]S. Hernandez, N. Blanco, I. Martil, G. Gonzalez-Diaz, R. Cusco, and L. Artus, J. Appl. Phys. **93**, 9019 (2003).
[7]J. Wagner, M. Peter, K. Winkler, and K. H. Bachem, J. Appl. Phys. **83**, 4299 (1998).
[8]J. Oshinowo, A. Forchel, D. Grutzmacher, M. Stollenwerk, M. Heuken, and K. Heime, Appl. Phys. Lett. **60**, 2660 (1992).
[9]W. P. Gillin, S. S. Rao, I. V. Bradley, K. P. Homewood, A. D. Smith, and A. T. R. Briggs, Appl. Phys. Lett. **63**, 797 (1993).
[10]F. Bollet, W. P. Gillen, M. Hopkinson, and R. Gwilliam, J. Appl. Phys. **93**, 3881 (2003).
[11]G. J. van Gurp, W. M. van de Wijgert, G. M. Fontijn, and P. J. A. Thijs, J. Appl. Phys. **67**, 2919 (1990).
[12]K. Nakashima, Y. Kawaguchi, Y. Kawamura, Y. Inamura, and H. Asahi, Appl. Phys. Lett. **52**, 1383 (1988).
[13]K. Kurishima, T. Kobayashi, and U. Gosele, Appl. Phys. Lett. **60**, 2496 (1992).
[14]S. A. Schwartz, P. Mei, T. Venkatesan, R. Bhat, D. M. Hwang, C. L. Schwartz, M. Koza, L. Nazar, and B. J. Skromme, Appl. Phys. Lett. **53**, 1051 (1988).
[15]H. Temkin, S. N. G. Chu, M. B. Panish, and R. A. Logan, Appl. Phys. Lett. **50**, 956 (1987).
[16]I. Rasnik, M. J. S. P. Brasil, F. Cerdeira, C. A. C. Mendonca, and M. A. Cotta, J. Appl. Phys. **87**, 1165 (2000).
[17]P. Ebert, M. Heinrich, M. Simon, K. Urban, and M. G. Lagally, Phys. Rev. B **51**, 9696 (1995).
[18]⟨http://www.gel.usherb.ca/casino/index.html⟩
[19]S. A. Campbell, *The Science and Engineering of Microelectronic Fabrication* (Oxford University Press, New York, 1996).
[20]H. Ikeda, Y. Miura, N. Takahashi, A. Koukitu, and H. Seki, Appl. Surf. Sci. **82/83**, 257 (1994).
[21]Z. Sobiesierski, D. I. Westwood, P. J. Parbrook, K. B. Ozanyan, M. Hopkinson, and C. R. Whitehouse, Appl. Phys. Lett. **70**, 1423 (1997).
[22]N. Kobayashi and Y. Kobayashi, J. Cryst. Growth **124**, 525 (1992).
[23]O. Kubaschewski and P. J. Spencer, *Materials Thermochemistry* (Butterworth-Heinemann, London, 1993).
[24]D. K. Gaskill, N. Bottka, L. Aina, and M. Mattingly, Appl. Phys. Lett. **56**, 1269 (1990).